https://doi.org/10.2352/EI.2026.38.16.AVM-111

Recommendations for Road Markings to Improve Machine Vision in Autonomous Driving

Brian Deegan[1,2] and Robin Jenkin[3]

[1]Dept. of Electrical & Electronic Engineering, University of Galway, Ireland
[2]Lero, the Research Ireland Centre for Software, Ireland
[3]NVIDIA, Santa Clara, California, USA

Abstract

Road markings have been standardized for human perception for over a century. With the rapid expansion of autonomous vehicles that rely on machine vision, new challenges emerge: markings optimized for human drivers may fail automated perception systems under low lighting, adverse weather, or high retroreflectivity conditions. Drawing on imaging science, vehicle dynamics, and experimental results from road-paint sample analysis, we identify four critical design factors, including spatial characteristics, color, contrast, and retroreflectivity, and provide concrete recommendations for evolving road marking standards. These augment rather than replace existing human-centric requirements and are developed in alignment with the IEEE P2020 Automotive Image Quality Standards working group.

Introduction

For generations, road markings and related infrastructure have been designed with human perception in mind. All governing standards have been calibrated around the capabilities of human vision. Roads are now shared between human drivers and increasingly sophisticated autonomous systems, robotaxis, assisted-driving platforms, and fully automated vehicles, creating a pressing need to revisit whether current marking designs serve both user types equally.

The challenge is not that human and machine requirements are fundamentally opposed; rather, machine vision imposes additional constraints that human-centric standards do not capture. A marking that guides a human driver perfectly in daylight may be invisible to a camera at night, or so intensely retroreflective that it causes overexposure and destroys color information. Critically, improvements for machine vision must not compromise human safety: a material that aids algorithm performance must not create a slipping hazard or impair legibility for human drivers.

This paper addresses four critical factors: *spatial characteristics*, *color*, *contrast*, and *retroreflectivity*. We draw on Johnson's imaging criteria, MTF/PSF analysis, European and US regulatory frameworks, and experimental paint-sample characterization to develop actionable recommendations for standards bodies, including CEN TC 226, FHWA, and IEEE P2020.

Regulatory Context

Three major frameworks govern road marking performance internationally. In Europe, EN 1436 defines performance classes for luminance factor, retroreflectivity (dry and wet), skid resistance, and color. In the United States, the MUTCD (FHWA) governs markings, with ASTM D6628 (color), ASTM E1710 (retroreflectivity), and ASTM E2177 (wet retroreflectivity) as associated material standards. Table 1 summarizes the principal parameters of both frameworks.

Table 1: Key parameters: European, US, and Chinese road marking standards [1, 2, 3, 4].

Parameter	Europe	USA	China
Standards	EN 1436, EN 1463	MUTCD, ASTM E1710	GB 5768.3, GB/T 16311
White $\beta_{\min}$	0.30 (Q2)	0.40	0.30
Yellow $\beta_{\min}$	0.27	0.27	0.27
Centre-line color	White	Yellow	Yellow
Temp. color	Yellow	Orange	Orange
RL system	Classes R0–R5	Min. thresholds	Min. thresholds
Min. RL (motorway)†	≥200	≥250	≥100
Wet RL	RW classes mandated	State-level only	Not mandated
Skid resistance	Classes S0–S5	State-specified	Not specified

†Units: $\mathrm{mcd\,m^{-2}\,lx^{-1}}$

A third major framework is the Chinese national standard series GB 5768 [3], which governs road markings on all public roads in the People's Republic of China. The pavement marking specification and test method is codified in GB/T 16311 [4], most recently updated in 2024. Like the European and US frameworks, GB/T 16311 restricts pavement markings to white and yellow, with color defined by CIE chromaticity polygons and minimum luminance factors ($\beta \geq 0.30$ for white, $\beta \geq 0.27$ for yellow) [5]. The color-semantic convention aligns with the US scheme: yellow longitudinal lines separate opposing traffic flows, while white lines separate same-direction lanes and delineate the right edge [3]. Orange markings are reserved for temporary work-zone guidance, consistent with US practice but opposite to the European yellow-temporary convention [6]. Retroreflectivity is specified via absolute minimum thresholds (rather than EN 1436's tiered class system), with the standard 30-meter measurement geometry from GB/T 21383, now essentially identical to that of ASTM E1710 and EN 1436, facilitating cross-regional comparison [4]. Wet-condition retroreflectivity and skid resistance are not mandated at the national level, representing a notable gap relative to EN 1436. These differences are summarized alongside the European and US frameworks in Table 1.

All three frameworks define color using CIE chromaticity polygons, calibrated to the standard human observer. This presents an immediate challenge for machine vision systems, which increasingly use non-Bayer color filter array (CFA) patterns such as RYYCY, RCCB, and RCCG. Such sensors have different spectral responses to the CIE observer, potentially causing metameric failures where colors that appear identical to a human look different to a camera, or vice versa.

One of the most operationally significant cross-regional differences is the semantic meaning of color. In the US, yellow marks permanent center lines separating opposing traffic; in Europe, yellow signals temporary deviations due to roadworks, with orange used in the US for the same purpose. These conventions have direct implications for autonomous systems trained on data from one region and deployed in another.

There are also structural differences in how retroreflectivity is specified. EN 1436 employs a formal class system (R0–R5 dry, RW0–RW3 wet), allowing road authorities to select a performance tier proportional to road type and speed. The US framework specifies absolute minimum thresholds by road type: freeway white edge lines require $\geq 250\,\mathrm{mcd\,m^{-2}\,lx^{-1}}$; rural arterials $\geq 100\,\mathrm{mcd\,m^{-2}\,lx^{-1}}$. Despite the structural differences, the numerical values align closely with EN 1436 classes R4–R5 and R1 respectively, suggesting a practical convergence that provides a foundation for harmonization. The 30-meter measurement geometry is now essentially identical in both EN 1436 and ASTM E1710, enabling direct cross-jurisdictional comparison.

Skid resistance is another area with important implications for any novel marking design. EN 1436 defines SRT classes S0–S5 (British Pendulum Tester values from no requirement to ≥ 65). Whatever recommendations are made for machine-vision-optimized markings, they must not reduce the frictional performance of the road surface. A material that improves camera detectability but creates a slipping hazard is not acceptable. This constraint applies equally to any new pigments introduced to address spectral separability and to any structured surface treatments introduced to improve contrast.

The three frameworks reviewed above sit beneath a common international umbrella: the Convention on Road Signs and Signals concluded in Vienna on 8 November 1968 and in force since 6 June 1978 [7]. The Convention establishes the foundational principle that pavement markings shall be white or yellow, and specifies basic line-type rules (broken lines for lane division, solid lines reserved for restricted-crossing situations) and a 6 mm height limit on raised elements [7]. Crucially, it sets no quantitative photometric thresholds: luminance factor, retroreflectivity, and skid resistance are delegated entirely to domestic or regional technical instruments, which accounts for the structural divergence between EN 1436, the MUTCD/ASTM suite, and GB 5768/GB/T 16311 described above. The Convention currently has 71 contracting parties, predominantly in Europe, Africa, the Middle East, and parts of Asia and Latin America; neither the United States nor the People's Republic of China is a signatory [8], meaning both nations develop their marking regimes independently of the treaty framework. For machine-vision systems intended for cross-regional deployment, this non-participation is significant: it removes any treaty-level guarantee of marking color consistency and reinforces the need to treat each jurisdiction's standard as an independent input to sensor and algorithm design.

Table 2: Johnson criteria for visual discrimination tasks.

Task	**Cycles** N	**Pixels**
Detection	1.0	2
Orientation	1.4	≈3
Recognition	4.0	8
Identification	6.4	≈13

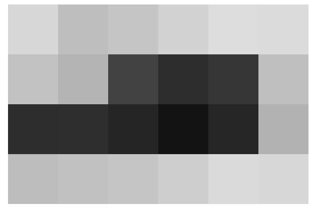

(a) One cycle (detection)

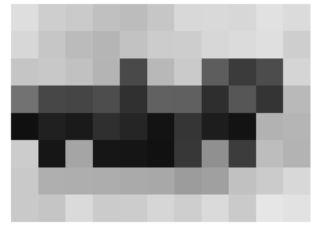

(b) Two cycles (orientation)

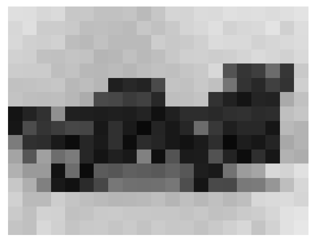

(c) Four cycles (recognition)

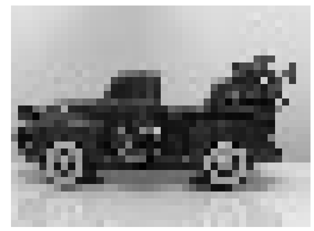

(d) Eight cycles (identification)

Figure 1: Johnson criteria for detection, orientation, recognition and identification

Spatial Characteristics

Appropriate road marking dimensions for machine vision can be derived from first-principles reasoning drawn from established imaging science.

Johnson Criteria

John Johnson (1958) experimentally determined the number of spatial frequency cycles required on an object to perform specific visual discrimination tasks [9], summarized in Table 2. These criteria provide a principled basis for specifying the minimum resolvable size of road markings as a function of camera parameters and detection distance. These criteria are usually simplified to 1, 2, 4, and 8 cycles. Empirical evidence from machine vision systems closely matches the original framework: with approximately 16 pixels on target, detection and classification tend to work reliably, as illustrated in Fig. 1.

Linking Criteria to Camera Parameters

Using the thin-lens formulation, the number of cycles N resolved on an object of height h_o at range r, with focal length f and pixel size p, is:

$$N = \frac{h_o f}{2 p r} \tag{1}$$

Rearranging to solve for the minimum required marking height at a given detection range:

$$h_o = \frac{2 N p r}{f} \tag{2}$$

This relationship has been validated experimentally. Using an f/2.4 lens with $p = 1.12\,\mu\mathrm{m}$ pixels and a 56° field of view, individual letters of height 20.3 cm yield approximately 1.0 cycle at 300 m (detectable), 4.7 cycles at 150 m (readable), and 8.9 cycles at 80 m (fully identifiable). This aligns closely with the predicted Johnson transitions and observed image clarity.

Range from Vehicle Dynamics

The detection range r for which markings must remain legible is bounded by the vehicle's stopping distance. For velocity V, system latency L, maximum deceleration D, and jerk J (rate of deceleration onset), the stopping distance d is:

$$d = VL + \frac{V^2}{2D} + \frac{VD}{2J} \tag{3}$$

Adding a safety cushion factor k and substituting d for r in Eq. (2) yields:

$$h_o = \left(VL + \frac{V^2}{2D} + \frac{VD}{2J} \right) \frac{2kNp}{f} \tag{4}$$

This directly links road marking height specifications to speed limits and vehicle dynamics, providing a principled, auditable derivation of spatial standards.

Effective Resolution: PSF Analysis

Johnson's formulation uses pixel pitch p as the resolution unit, but the effective resolution of a real camera is governed by the system point spread function (PSF), not pixel size alone. A more accurate estimate multiplies the MTF contributions of optics, pixel aperture, and motion blur, then takes the inverse Fourier transform to obtain the PSF. The full-width of the PSF at the noise floor gives the effective pixel size p_{eff} to substitute in Eq. (2).

For example, an f/1.6 lens with $p = 2.1\,\mu$m pixel pitch produces a PSF width of approximately $2.84\,\mu$m. This is broader than the nominal pixel pitch, due to diffraction and aperture convolution. At highway speeds, motion blur further broadens the PSF. Substituting p_{eff} into Eq. (2) yields more conservative and realistic predictions of marking detectability, which is particularly important at high vehicle speeds.

Recommendation: Derive road marking spatial specifications by combining Johnson criteria with PSF-based effective resolution and vehicle stopping distance, updated for realistic optics and motion blur.

Contrast

For either a human driver or a machine vision algorithm to detect lane markings, those markings must have sufficient contrast against the road surface. What level of contrast is required, and how to standardize it, remains an open question.

In regions where road surfaces are constructed from light-colored materials (pale concrete, limestone chip seal), white paint against a very light surface can be nearly invisible, particularly under bright overhead lighting or on wet roads. Machine vision systems tuned to detect the white-dark boundary of a lane line fail entirely when both sides of the boundary are near-white.

A promising solution already deployed in some US states is the Contrast Pavement Marking (CPM): a retroreflective white line flanked by a non-retroreflective black border (Fig. 4). The black element ensures a detectable luminance transition regardless of surface color, and preliminary evidence suggests this approach works well under adverse conditions and low-sun angles.

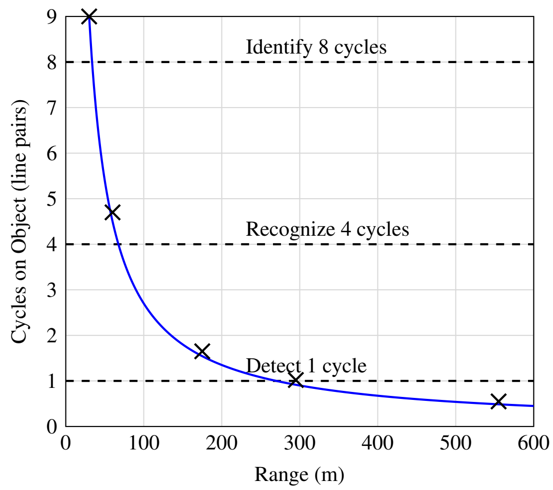

Johnson criteria for an *f/2.4, 3264×2448, 1.12 µm pixel, 56 degree field of view camera, 20.3 cm text*

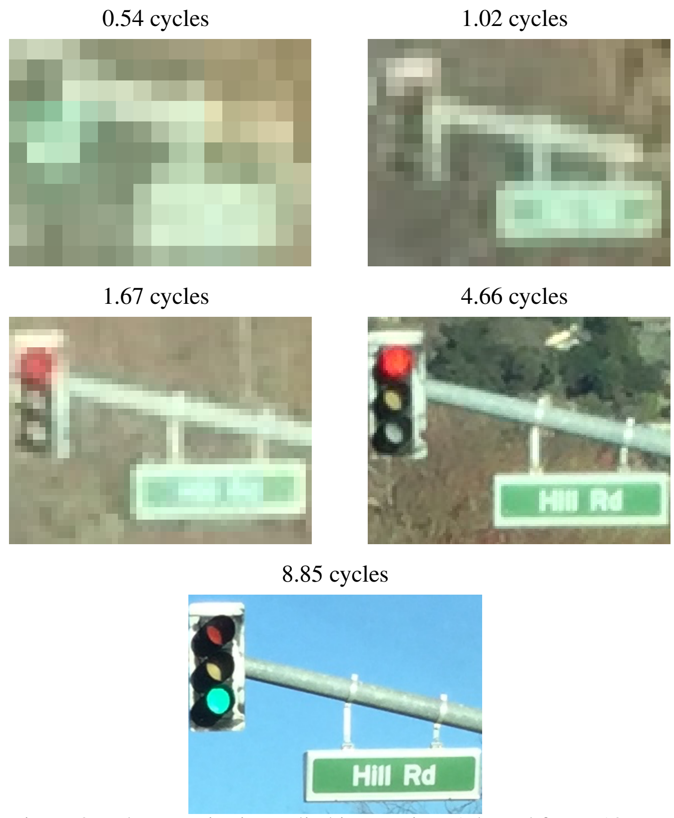

Figure 2: Johnson criteria applied in practice. Adapted from [10]

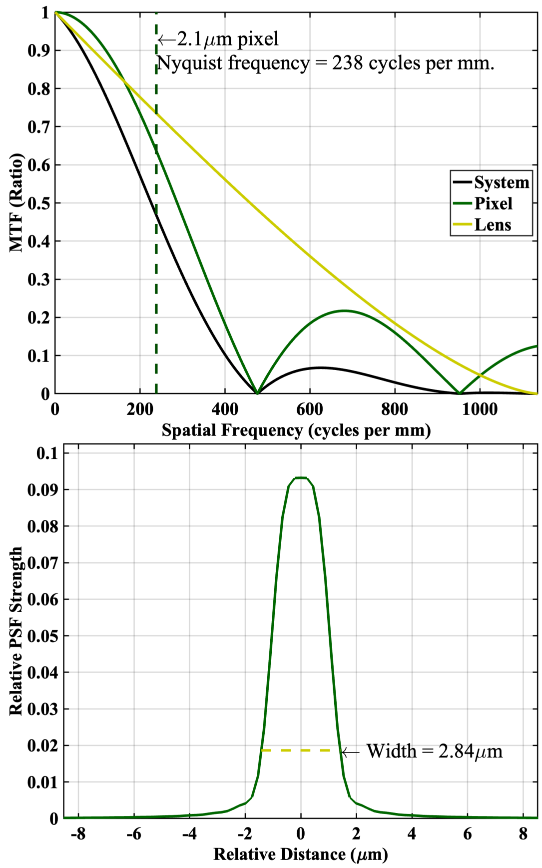

Figure 3: Theoretical PSF and MTF of diffraction limited F1.6 lens and 2.1 μm pixel pitch

However, CPM designs are not yet standardized. Implementations vary in border width, relative positions, and inner/outer arrangements. Behavior under motion blur at highway speed, where the spatial frequency of the black-white boundary determines detectability, has not been systematically characterized. Open questions include: what is the optimal ratio of black border width to white line width? How do the two components merge under motion blur at different vehicle speeds? Does the arrangement (black outside white, or alternating black-white-black) affect detection by machine vision algorithms differently from human perception?

There is also the question of orange-yellow separation. In the US system, orange temporary markings and yellow permanent markings must be reliably distinguished by autonomous systems. Under certain illuminants and with non-Bayer sensors, the chromaticity difference between these two colors may be insufficient for reliable classification. The CIE color boxes for orange and yellow are adjacent in chromaticity space, and the existing tolerance polygons were not designed with the diversity of modern automotive sensors in mind.

Recommendation: Introduce minimum contrast ratio requirements between markings and the road surface. Standardize CPM geometry (border width, arrangement, and minimum luminance ratio) for deployment on light-surface roads. Investigate and, if necessary, increase the chromaticity separation between orange and yellow marking standards.

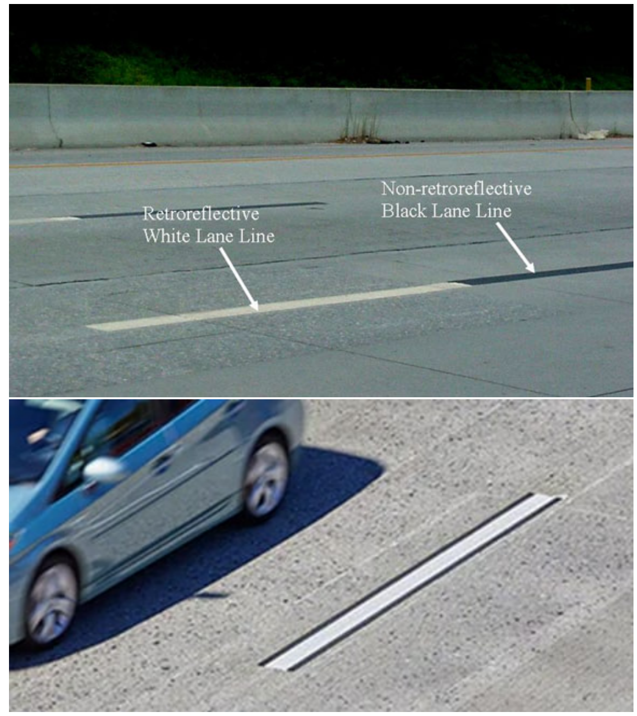

Figure 4: Plain white marking vs. Contrast Pavement Marking (CPM) with black borders, on light-colored road surface [11, 12]

Color and Spectral Considerations

Road marking colors are specified using CIE chromaticity coordinates (x, y), defining tolerance polygons calibrated to the CIE 1931 standard observer. Manufacturers are required to produce paints whose color falls within these polygons; however, the spectral means of achieving compliance are unconstrained.

This presents a growing problem. Automotive cameras increasingly use non-standard CFA patterns: RYYCY (adding yellow-filtered pixels), RCCB (replacing green with clear), RCCG, and others. These sensors sample the spectrum differently from the standard Bayer (RGGB) pattern. A paint whose chromaticity falls within the EN 1436 yellow polygon under D65 illumination may appear indistinguishable from orange to a non-Bayer sensor or may appear differently across camera models, even when both are individually compliant.

The core issue is *metamerism*: two surfaces with different spectral reflectance functions can have identical CIE chromaticity coordinates under one illuminant/observer combination yet look different under another. As automotive cameras diversify in spectral response, chromaticity-only specifications become insufficient to guarantee color separation.

The RCCB Discrimination Problem

The mechanism of failure is concrete. In a standard Bayer sensor, the green channel (peaking near 540 nm) is the primary discriminant between yellow and orange road markings. Yellow pigments (organic or chrome-based) exhibit high reflectance above approximately 530 nm, while orange pigments transition to high reflectance only above approximately 575 nm. The reflectance difference in the 530–580 nm band reaches a maximum near 550 nm, where $\Delta R \approx 0.47$ between representative yellow and orange paints, as shown in Fig. 5. The Bayer green channel inte-

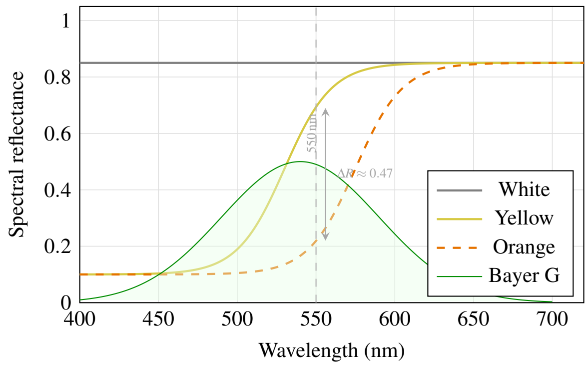

Figure 5: Representative spectral reflectance of white, yellow, and orange road marking paints under D65. The Bayer green channel sensitivity (shaded, scaled for overlay) is centred on the 530–580 nm region where yellow and orange diverge most. The maximum reflectance separation of $\Delta R \approx 0.47$ occurs near 550 nm. Sensors lacking a spectrally selective green channel (e.g. RCCB) lose access to this discriminating region.

grates directly over this region, yielding a G/R ratio of 0.73 for yellow versus 0.48 for orange, a separation of 0.25 that is robust to normal measurement variation.

In an RCCB sensor, the green channel is replaced by a panchromatic clear channel with a flat response across the visible spectrum. The clear channel integrates the same 530–580 nm signal, but equally integrates the 580-700 nm region, where both yellow and orange reflect similarly. The resulting C/R ratio is 1.49 for yellow versus 1.35 for orange, a separation of only 0.14, approximately 56% of the Bayer discrimination. RYYCY sensors, which add a yellow-filtered channel peaking near 590 nm, fare similarly: the Y/R ratio yields a separation of approximately 58% of Bayer. The problem is structural: any sensor lacking a spectrally selective channel centered in the 530–580 nm window will underperform on yellow/orange discrimination, regardless of its overall sensitivity or dynamic range.

A Sketch of Spectral Specification

The practical implication is that compliant paints, i.e., those whose chromaticity coordinates (x,y) fall within the EN 1436 or ASTM D6628 polygons, may nonetheless fail to provide adequate spectral separation for non-Bayer sensors. Two manufacturers can produce chromaticity-compliant yellow paints with spectral reflectance curves that differ substantially in the 530-580 nm region, depending on pigment class (organic diarylide, chrome yellow, iron oxide). A camera with a spectrally selective green channel will discriminate both from orange; a camera without one may not.

The solution is to supplement existing chromaticity polygons with *checkpoint reflectance values* at a small number of diagnostic wavelengths. These checkpoints do not replace the chromaticity requirement; they add a spectral constraint beneath it, with minimal additional measurement complexity. Table 3 presents a proposed set of checkpoints for the four primary road marking colors. Two visible-band checkpoints and one NIR checkpoint per color class suffice to constrain the spectral shape without requiring full spectrophotometric measurement.

The critical checkpoint is $R(550\,\text{nm})$. Yellow paint must achieve $R(550\,\text{nm}) \geq 0.55$, while orange must remain below 0.40;

Table 3: Proposed spectral reflectance checkpoints to supplement existing CIE chromaticity requirements. Values are indicative; calibration against a measured reference pigment database is needed before adoption. Measurement geometry: 45/0, D65 illuminant, matching existing EN 1436 practice. The NIR checkpoint at 850 nm addresses non-visible automotive sensing.

Color	R**(550 nm)**	R**(650 nm)**	R**(850 nm)**
White	≥ 0.75	≥ 0.75	≥ 0.80
Yellow	≥ 0.55	≥ 0.80	0.40–0.80
Orange	≤ 0.40	≥ 0.75	—
Green	≥ 0.35	≤ 0.20	—

the 0.15-unit gap between the thresholds is sufficient to survive typical paint weathering and retroreflectometer measurement uncertainty. The $R(650\,\text{nm})$ checkpoint confirms that both yellow and orange achieve the expected high-reflectance plateau in the red band, excluding atypical pigments that satisfy chromaticity requirements through unusual spectral combinations. The $R(550\,\text{nm})$ checkpoint for green (school zone) markings confirms the presence of adequate green-band reflectance; the $R(650\,\text{nm})$ upper bound ensures the marking remains spectrally distinct from yellow in the red channel.

The NIR checkpoint at 850 nm for white and yellow addresses a distinct failure mode. White paint (TiO_2-based) is highly NIR-reflective, with $R(850\,\text{nm}) \approx 0.85$–$0.95$, whereas yellow paints vary substantially depending on pigment: organic diarylide yellows typically yield $R(850\,\text{nm}) \approx 0.40$–$0.60$, while chrome yellow ($PbCrO_4$) can reach 0.70–0.85. Two chromaticity-compliant yellow paints can therefore differ by up to 0.40 in NIR reflectance, making NIR-based lane classification unreliable not because yellow and white are intrinsically similar in NIR, but because current standards do not constrain NIR behavior at all. An indicative range of 0.40–0.80 is proposed for yellow, pending measurement against a reference pigment database.

The measurement infrastructure required is modest. Spectrophotometers capable of reporting $R(\lambda)$ at 550, 650, and 850 nm are standard equipment in road marking quality laboratories. The 45/0 geometry already mandated by EN 1436 for luminance factor measurement is appropriate for spectral checkpoint measurement. A necessary next step would be measuring the full spectral reflectance of materials currently in service and compliant with EN 1436 and ASTM D6628, to confirm that the proposed thresholds accommodate the legitimate range of compliant pigments without inadvertently excluding them. This is a standardization task, not a research task; CIE Technical Committee work on road surface photometry provides a natural home for it.

Retroreflectivity and Camera Overexposure

Road markings contain glass microspheres that return incident headlight energy toward the driver, enabling nighttime visibility. Current standards mandate minimum retroreflectivity levels: EN 1436 classes R1-R5 in Europe; FHWA threshold values in the US. However, the same property introduces a specific hazard for automotive camera systems.

Retroreflectivity Classes

EN 1436 defines six dry-night retroreflectivity classes and four wet-night classes, shown in Table 4. These classes allow

Table 4: EN 1436 retroreflectivity classes (R_L in $\mathrm{mcd\,m^{-2}\,lx^{-1}}$, 30-m geometry).

Class	**Dry R_L**	**Wet R_W**	**Application**
R0/RW0	No req.	No req.	No night req.
R1/RW1	$\geq$100	$\geq$35	Urban roads
R2/RW2	$\geq$150	$\geq$50	Rural roads
R3/RW3	$\geq$200	$\geq$75	Motorways
R4	$\geq$300	—	Enhanced
R5	$\geq$400	—	Premium

road authorities to specify performance requirements proportional to road type and design speed. Motorways are typically specified at R3 dry / RW2 wet; rural roads at R2 / RW1; urban roads at R1 or R2 / RW0 or RW1. Wet-night performance is achieved through glass bead protrusion above the marking film: microspheres must remain partially exposed above the water film surface to function retroreflectively.

Dynamic Range and Overexposure

Standard cameras offer approximately 60 dB of dynamic range per exposure; automotive cameras are designed for 120 dB or more. Despite this, highly retroreflective markings at close range under headlights can still drive pixels into saturation. When pixels are overexposed, raw sensor values carry no meaningful color information, defaulting to a white-clipped response regardless of the marking's actual color. The result is a systematic loss of color separation: a direct failure mode for color-based lane classification.

Experimental Evidence

Paint samples representing green (school zone), yellow, and white road marking paints with varying glass bead concentrations were prepared and imaged to characterize the effect of retroreflective overexposure on color separability. Twelve samples were used in total: three green, three white, and six yellow, with three levels of retroreflective bead concentration applied across each color group. Samples were imaged using an Apple iPhone 12 under two illumination conditions: flash off (ambient only) and flash on (simulating the directional retroreflective return from vehicle headlights). Ambient lighting was provided by a 5000 K CCT LED source at 100 lux. The experimental images are shown in Fig. 6.

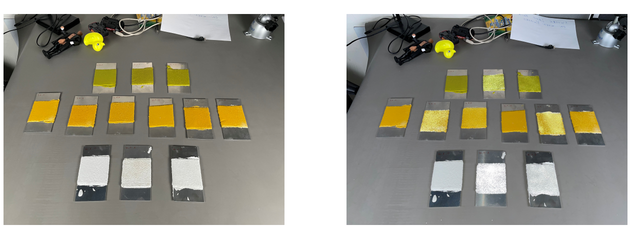

(a) Flash Off (b) Flash On

Figure 6: Examples of white, yellow and green road paint samples with varying amounts of retroreflective material

Without flash illumination, samples were easily classified: green, yellow, and white formed well-separated clusters in RGB color space with large inter-cluster distances (Table 5). With flash illumination activating the retroreflective beads, the color distributions of yellow and green samples converged dramatically. The Mahalanobis distance [13] between green and yellow dropped from 93.0 to 4.4, a reduction in discriminability of more than an order of magnitude.

Table 5: Color distance metrics for selected patch pair comparisons under flash-on and flash-off conditions

Condition	Patch Pair	Euclidean Distance	Mahalanobis Distance	ΔE_{76}
Flash On	2 vs. 5	16.90	4.21	6.81
	2 vs. 11	141.97	33.61	50.11
	5 vs. 11	136.08	24.36	49.48
Flash Off	2 vs. 5	67.24	66.24	24.22
	2 vs. 11	198.30	57.28	54.69
	5 vs. 11	173.64	82.57	61.35

This result is significant: a camera encountering highly retroreflective yellow and green markings under headlight illumination may be statistically unable to classify them correctly, confusing school zone green markings with standard yellow center lines. Both traditional and deep-learning-based classification algorithms rely on consistent color distributions; overexposure breaks this assumption at the sensor level.

Proposed Maximum Retroreflectivity Limit

Recommendation: Road marking standards should define both minimum and *maximum* retroreflectivity limits. The minimum ensures nighttime visibility for human drivers; the maximum prevents camera overexposure and color separation loss. The specific ceiling value will require further empirical research across headlight intensities, camera apertures, and sensor dynamic ranges, but the principle is well-supported by the experimental data and represents a clear gap in current standards.

Summary of Recommendations

Table 6 consolidates the recommendations arising from this analysis. These are proposed for consideration by CEN TC 226, FHWA, and the IEEE P2020 working group.

Discussion

The recommendations above are augmentations of existing standards, not replacements. A marking correctly sized for machine detection at highway speeds is also larger and more visible to humans. A marking whose retroreflectivity is bounded from above remains fully visible to human drivers at night while no longer causing camera saturation. Contrast borders benefit both human and machine perception on light-surface roads.

The more structurally challenging recommendation is the introduction of spectral definitions. This requires coordination with paint manufacturers, test equipment suppliers, and standards bodies. The CIE chromaticity framework is deeply embedded in existing practice; supplementing rather than replacing it is the pragmatic path. A necessary first step would be standardization of spectral reflectance measurement methods for road markings under representative illuminants, including D65 and automotive LED headlight spectra. CIE Technical Committee work on automotive lighting metrology provides a relevant framework that could be extended to marking materials.

There are areas of emerging convergence between European and US standards. The 30-meter retroreflectometer geometry

Table 6: Summary of recommendations for road marking standards.

Topic	Recommendation
Spatial design	Derive marking dimensions from Johnson criteria combined with PSF-based effective resolution and vehicle stopping distance.
Spectral defs.	Add spectral reflectance definitions alongside CIE chromaticity polygons to address non-Bayer sensor metamerism.
Contrast	Mandate minimum marking-to-surface contrast ratio; standardize CPM (black-border) geometry for light-surface roads.
RL bounds	Define both minimum and maximum retroreflectivity limits to balance nighttime visibility with camera dynamic range.
Orange/yellow sep.	Increase chromaticity separation between US temporary orange and yellow to reduce misclassification risk.
Maintenance	Tighten in-service maintenance requirements; line discontinuities cause systematic failures in autonomous perception.
Symbol research	Investigate optimal symbol geometries for algorithmic detectability under motion blur and rolling shutter effects.

is now essentially identical in EN 1436 and ASTM E1710, enabling direct cross-jurisdictional measurement comparison. The numerical R_L thresholds for high-speed roads in FHWA guidance align closely with EN 1436 R3–R4 values. ASTM Committee E17.23 and CEN TC 226 have engaged in bilateral technical exchanges, and future revisions of ASTM D6628 are expected to reference D65 illuminant alongside Illuminant C, further aligning chromaticity measurement practice. These commonalities suggest that additional alignment on machine-vision-relevant parameters is achievable within existing standards structures.

An open question not fully addressed here is *maintenance*. Autonomous perception systems rely on consistent line presence and quality; a faded or partially missing marking that a human driver fills in from context may cause systematic failures in a lane-keeping algorithm. Stricter in-service maintenance schedules, combined with retroreflectivity-inclusive inspection protocols, would directly benefit autonomous system reliability. Current EN 1436 in-service requirements vary by member state; a harmonized minimum maintenance standard with machine-vision performance criteria could be a valuable addition.

Finally, the design of road *symbols*, including school zone markings, speed limit numerals, directional arrows, and yield signs, warrants dedicated study. The optimal stroke width, aspect ratio, and gap-to-stroke ratio for human legibility need not be the same as for machine classification, particularly when motion blur and rolling shutter effects are considered at highway speeds. This is an area where further research, guided by the spatial framework presented in Section 3, could yield concrete improvements to current symbol design standards.

Conclusion

Road markings standardized for human perception are increasingly relied upon by autonomous vehicle perception systems with fundamentally different sensor characteristics. This paper identified four critical gaps: (i) no formal link between marking spatial dimensions, camera parameters, and vehicle dynamics; (ii) chromaticity-only color definitions that fail with non-Bayer sensors; (iii) no minimum contrast ratio standards; and (iv) absence of retroreflectivity upper bounds, creating overexposure risk.

Practical, physics-grounded tools exist to address each gap. Johnson criteria combined with PSF-based resolution and vehicle dynamics equations provide a principled framework for spatial specifications. Spectral reflectance supplements to existing chromaticity polygons can address sensor diversity. Standardized CPM geometry would formalize a proven contrast approach. Upper retroreflectivity limits, informed by camera dynamic range and the experimental data presented, would address a demonstrable color separation failure mode.

These recommendations are offered as contributions to the IEEE P2020 working group and as input to future revisions of EN 1436, MUTCD, and associated standards, with the goal of creating roads that reliably and safely guide both humans and machines.

References

[1] European Committee for Standardisation (CEN). EN 1436:2018 - Road marking materials: Performance for road markings, 2018.

[2] Federal Highway Administration (FHWA). Manual on Uniform Traffic Control Devices (MUTCD). Technical report, US DOT, Washington, DC, 2023.

[3] Standardization Administration of China. GB 5768.3–2009: Road Traffic Signs and Markings—Part 3: Road Traffic Markings, 2009.

[4] General Administration of Quality Supervision, Inspection and Quarantine of the People's Republic of China. GB/T 16311–2024: Specification and Test Method for Road Traffic Markings, 2024. Previous edition: GB/T 16311–2009, implemented 2010-04-01.

[5] H. Liu, Y. Zhang, Y. Liao, J. Yuan, and Y. Guo. Investigating the daytime visibility requirements of pavement marking considering the influence of CCT and illuminance of natural light. *Int. J. Environ. Res. Public Health*, 19(5):3051, 2022.

[6] Standardization Administration of China. GB 5768.3–2025: Traffic Signs and Markings—Part 3: Traffic Markings, 2025.

[7] United Nations. Convention on Road Signs and Signals, 1968. Concluded at Vienna, 8 November 1968; in force 6 June 1978. United Nations Treaty Series, Vol. 1091, No. 16743.

[8] United Nations Treaty Collection. Chapter XI-B-20: Convention on Road Signs and Signals—Status of Treaty, 2024.

[9] J. Johnson. Analysis of image forming systems. In *Proc. Image Intensifier Symposium*, pages 244–273, Fort Belvoir, VA, 1958. US Army.

[10] R. Jenkin and P. Kane. Fundamental imaging system analysis for autonomous vehicles. In *IS&T International Symposium on Electronic Imaging Science and Technology*. Society for Imaging Science and Technology, 2018.

[11] 3M Company. Creating safer roads & highways for drivers. 3M Road Safety, 2024. [Online]. Available: `https://www.3m.com/3M/en_US/road-safety-us/applications/roads-and-highways/` [Accessed: Mar. 29, 2026].

[12] Texas Department of Transportation. Contrast markings. Section 4: Pavement Marking Material Descriptions. [Online]. Available: `https://www.txdot.gov/manuals/trf/pmh/`

material_selection/pavement_marking_material_descriptions-i1020814/contrast_markings.html. [Accessed: Mar. 29, 2026].

[13] R. Jenkin. Mahalanobis distance as a robust color (signal) separation metric. In *IS&T International Symposium on Electronic Imaging Science and Technology*. Society for Imaging Science and Technology, 2026.

Author Biography

Brian Deegan received his Bachelor's degree in Computer Engineering and M.Sc. in Biomedical Engineering from the University of Limerick in 2004 and 2005, and his Ph.D. in Biomedical Engineering from the University of Galway in 2011. He worked at Valeo Vision Systems from 2011 to 2022 as a Vision Research Engineer focused on image quality. In 2022, he joined the University of Galway as a Lecturer. His research interests span cerebral blood flow, HDR imaging, LED flicker, and machine-vision image quality.

Robin B. Jenkin received the BSc in imaging science from the University of Westminster (1994) and the PhD in image processing from University College London (1996). He is a Distinguished Engineer at NVIDIA Corporation, where he models image quality for autonomous vehicle and other applications. Robin is a Fellow of The Royal Photographic Society, a Visiting Professor at the University of Westminster, and serves as Executive Vice President of the board of IS&T.